Nondiffusive Brownian motion of deformable particles: Breakdown of the "long-time tail"

Sándalo Roldán-Vargas,[1,*] Miguel Peláez-Fernández,[1] Ramon Barnadas-Rodríguez,[2,3] Manuel Quesada-Pérez,[4] Joan Estelrich,[2] and José Callejas-Fernández[1]

[1]*Departamento de Física Aplicada, Grupo de Física de Fluidos y Biocoloides, Universidad de Granada, E-18071 Granada, Spain*

[2]*Departament de Fisicoquímica, Facultat de Farmàcia, Universitat de Barcelona, Barcelona, E-08028 Catalonia, Spain*

[3]*Centre d'Estudis en Biofísica, Facultat de Medicina, Universitat Autònoma de Barcelona, Cerdanyola del Vallès Bellaterra, Barcelona, E-08193 Catalonia, Spain*

[4]*Departamento de Física, Escuela Politécnica Superior de Linares, Universidad de Jaén, Linares, E-23700 Jaén, Spain*

(Received 22 December 2008; revised manuscript received 3 July 2009; published 18 August 2009)

We study the nondiffusive Brownian motion of both rigid and deformable mesoscopic particles by cross-correlated dynamic light scattering with microsecond temporal resolution. Whereas rigid particles show the classical long-time tail prediction, the transition to diffusive motion of deformable particles presents a striking behavior not explained by the existing hydrodynamic treatments. This observation can be interpreted in terms of a damped oscillatory deformational motion on time scales of the order of the Brownian time. Finally, we show that the nondiffusive Brownian motion depends on the specific flexibility of the particles.

DOI: 10.1103/PhysRevE.80.021403 PACS number(s): 82.70.Dd, 05.40.Jc

The dynamics of a Brownian particle can be formulated on different levels of description depending on the time scale of interest and the refinement of the hydrodynamic approach [1–3]. Thus, in Einstein's classic investigation [4] no assumptions about the behavior of the particle velocity were made and the motion at long times of a "free" Brownian particle was shown to be diffusive. The initial attempt to incorporate velocity in the description of Brownian motion immediately came with the Langevin equation [5,6]. Within this approximation, the interaction between the particle and the surrounding fluid was separated into two forces associated with a common origin, a systematic friction and a fluctuating noise, with no considerations of hydrodynamic memory effects. Despite its mathematical significance, this simple model predicts an extremely fast transition from ballistic to diffusive motion which is found to be nonrealistic.

The true character of the transition from ballistic to diffusive motion was successfully explored by Alder and Wainwright [7,8] by means of molecular-dynamics simulations assuming a hard-sphere (HS) interaction. They found a "surprising persistence of the velocities" [8] through a "long-time tail" ($\propto \tau^{-3/2}$) in the velocity autocorrelation function, with the resultant delay in the emergence of the diffusive motion. In terms of macroscopic fluid dynamics, this observation was explained as a hydrodynamic memory effect due to the circulation of the fluid from the front of the particle, where the fluid is compressed, to the rear, where a rarefaction wave is developed. This vorticity effect pushes the particle resulting in a persistence of its motion. Soon, this finding was mathematically described by detailed hydrodynamics treatments [9–11] and the first real measurements of the long-time tail appeared for simple liquids [12,13]. For rigid colloidal particles, experiments using dynamic light scattering (DLS) [14–16], diffusing-wave spectroscopy [17,18], and optical trapping interferometry [19], have consolidated the existence of the long-time tail. Nevertheless, these studies have been based on the assumption of a HS-like interaction (computer simulations) or a fixed, rigid, geometrical shape of the tracer particles (experiments). However, despite their ubiquitous presence, a lack of these investigations devoted to deformable particles still persists.

In this paper, we use cross-correlated DLS to present experimental evidence against the validity of the classic long-time tail prediction in case of mesoscopic deformable particles suspended in a small-molecule solvent. Thus, as opposed to rigid particles, we document an original observation that can be interpreted in terms of the interplay between the translational and the deformational motion of our deformable particles on time scales of the order of the Brownian time. These data demand a complete theoretical approach to account for the nondiffusive Brownian dynamics of mesoscopic deformable particles. In absence of a theoretical understanding, we show that two deformable particles with similar diffusivity can be distinguished by their specific flexibility through their nondiffusive Brownian motion. As a result, our investigation appears as especially stimulating to be applied to mesoscopic biological objects whose functionality depends on their elastic properties to a great extent [20].

An essential relation holds for the isotropic motion of a Brownian particle between any Cartesian component of its mean-square displacement, $\langle \Delta x^2(\tau) \rangle$, and its corresponding velocity autocorrelation function, $\langle v_x(0) v_x(\tau) \rangle$ [6],

$$\langle \Delta x^2(\tau) \rangle = 2 \int_0^\tau (\tau - t) \langle v_x(0) v_x(t) \rangle dt. \tag{1}$$

The brackets denote ensemble averages. Equation (1) applied to the case of a Langevin's particle becomes [6]

$$\langle \Delta x^2(\tau) \rangle = 2D_0 [\tau - \tau_B + \tau_B \exp(-\tau/\tau_B)], \tag{2}$$

where D_0 is the particle's diffusion coefficient and $\tau_B = 2a^2\rho/9\eta$ the Brownian time. Here a and ρ represent the radius and density of a rigid mesoscopic spherical particle, whereas η is the shear viscosity of the fluid. In contrast, if

*Corresponding author. sandalo@ugr.es

we consider a complete hydrodynamic treatment including memory effects, Eq. (1) becomes [11,15]

$$\langle \Delta x^2(\tau)\rangle \cong 2D_0\left[\tau - 2\left(\frac{\tau_L}{\pi}\right)^{1/2}\tau^{1/2} + \frac{\tau_L}{9}\left(8 - \frac{2\rho}{\rho'}\right) - \frac{\tau_L^{3/2}}{9\sqrt{\pi}}\left(7 - \frac{4\rho}{\rho'}\right)\tau^{-1/2}\right]; \quad (\tau \geq \tau_L), \tag{3}$$

where $\tau_L=(9/2)(\rho'/\rho)\tau_B$, ρ' being the fluid density. Although both results, [Eqs. (2) and (3)] tend to a common diffusive regime, $\langle \Delta x^2(\tau)\rangle = 2D_0\tau$ $(\tau \gg \tau_B)$, the latter presents a slower transition due to its second term $(\propto \tau^{1/2})$, which is associated to the presence of the long-time tail $(\propto \tau^{-3/2})$ in $\langle v_x(0)v_x(\tau)\rangle$, as can be deduced from Eq. (1).

To test these theoretical predictions via DLS, an experimental determination of the normalized autocorrelation function of the scattered field $g_1(q;\tau)$ (q being the magnitude of the scattering vector) can be performed. In case of noninteracting, identical, and rigid spherical particles $g_1(q;\tau) = \langle \exp(iq\Delta x(\tau))\rangle$. If measurements of $g_1(q;\tau)$ are made at short times $(\tau \approx \tau_L)$, non-Gaussian effects are hardly appreciable regardless of the statistics of v_x, as can be proven by Taylor's expansion of $g_1(q;\tau)$ [15]. Accordingly [21],

$$g_1(q;\tau) = \exp\left(-\frac{1}{2}q^2\langle \Delta x^2(\tau)\rangle\right). \tag{4}$$

However, instead of using directly $g_1(q;\tau)$ to probe Eqs. (2) and (3), an experimental time-dependent "diffusion coefficient" $D_{\exp}(\tau) \equiv (-1/q^2)d \ln g_1(q;\tau)/d\tau$ is frequently defined [15,17]. As a result, the slopes of $\langle \Delta x^2(\tau)\rangle/2$ obtained from Eqs. (2) and (3) are compared with $D_{\exp}(\tau)$, which is determined by numerical differentiation. Nevertheless, we should note that whereas Eqs. (2) and (3) consider uniquely the theoretical translational motion, $D_{\exp}(\tau)$ could also reflect the motion corresponding to nontranslational degrees of freedom. This will be a central point in our discussion.

To obtain $D_{\exp}(\tau)$ for the suspensions investigated in this work, we used a three-dimensional DLS spectrometer (LS instruments, Fribourg, Switzerland) with two incident He-Ne laser beams ($\lambda = 632.8$ nm). Suspensions were contained in a cylindrical scattering cell which was immersed in a thermostatized bath. A digital correlator (Flex03lq-OEM) computes the normalized cross-correlation function, $g_C^2(q;\tau)$ of the registered scattered intensities detected by two avalanche photodiodes (SPCM-AQRH) for which the time-dependent contributions of multiple scattered photons can be neglected. The experimental $g_1(q;\tau)$ were obtained through the relation $g_C^2(q;\tau) = 1 + \beta[g_1(q;\tau)]^2$ $(0 < \beta < 1)$, with a similar protocol as that described in Ref. [22] for a two-color DLS scheme. The sample time resolved with our correlator is 12.5 ns, with 286 τ values along the interval $[1.25\cdot 10^{-8}, 10^{-4}]$ s. For all the experiments, photon counting rates were kept within $[10^5, 5\cdot 10^5]$ s^{-1} to ensure a maximum dead time of 40 ns, being always under the saturation limit. A reliable statistical estimator of $g_1(q;\tau)$ resulted from the average of 25 independent measurements with 1000 s per measurement. Thus, spurious determinations due to electronic distortions, even at delay times as short as 0.2 μs, are minimized. The magnitude of the scattering vector was fixed at $q_f = 0.026$ nm^{-1}.

For our experimental study, we used three different suspensions which were sufficiently diluted to avoid long-range interactions. First, an aqueous suspension of polystyrene microspheres, denoted as "sample R" (rigid), with mean radius $a_R = 650$ nm, relative standard deviation RSD=0.04, and particle volume fraction $\phi_R = 0.002\%$. The second sample, "sample D" (deformable), was an aqueous suspension of liposomes made of soybean phosphatidylcholine (SPC) from Lipoid, with mean external radius $a_D = 244$ nm, RSD=0.15, and $\phi_D = 0.01\%$. The third sample, "sample RD" (rigid-deformable), was an aqueous suspension of liposomes made of dimyristoylphosphatidylcholine (DMPC) from Sigma-Aldrich, Inc., with $a_{RD} = 242$ nm, RSD=0.15, and $\phi_{RD} = 0.01\%$. Due to the extrusion procedure, both SPC and DMPC liposomes show an unilamellar thickness of about 5 nm [23]. The twofold (rigid-deformable) behavior of sample RD comes from the composition of the lipid bilayers, since DMPC membranes exhibit two main phases separated by a threshold temperature (known as main transition temperature): a rigid gel phase and a deformable liquid crystalline phase. Below the main transition temperature, the DMPC membranes retain their rigidity. Above the main transition temperature, that is, in the liquid crystalline phase, it is considered that the majority of the single carbon-carbon bonds of the acyl chains of the lipid bilayers have free rotation [24]. This phenomenon evidences the conversion of the DMPC membrane from the gel to the liquid crystalline phase, where the membrane displays new properties such as an increased permeability and a fluidized state. Thus, we can treat sample RD as rigid or deformable by changing the temperature around its critical value. The main transition temperature of the DMPC bilayers was established at 23.0 ± 0.1 °C by means of differential scanning calorimetry [24].

Using the described protocol, two examples of the classic long-time tail prediction at 13 and 25 °C are shown in Figs. 1(a) and 1(b) for sample R. While Langevin's model does not predict the real evolution of $D_{\exp}(\tau)$, the full hydrodynamic model (without fitting parameters) and $D_{\exp}(\tau)$ show a good agreement. Thus, whereas at short times a significant contribution of the long-time tail term $(\propto \tau^{-1/2})$ is apparent, at moderate long times $(\tau \geq 40$ μs) the diffusive regime, $D(\tau)/D_0 \approx 1$, is nearly recovered. In addition, the time evolution of $D_{\exp}(\tau)$ corresponding to sample D at 25 °C is shown in Fig. 1(c): Neither Langevin's model nor the full hydrodynamic treatment describe satisfactorily these new experimental results. Now $D_{\exp}(\tau)$ shows a clear nonmonotonic behavior with at least two marked maxima within our time window over the corresponding Langevin's prediction. After reaching the second maximum $(\tau^* \approx 3.7$ μs), $D_{\exp}(\tau)$ decreases smoothly and tends to its diffusive value, D_0. Since their environments are similar, the distinct trends shown by $D_{\exp}(\tau)$ for the polystyrene spheres and the SPC liposomes should be caused by the different structural properties of these particles. To support this statement, we present the results obtained for sample RD at different temperatures around the main transition temperature. Thus, the unique significant change in the dynamics of this suspension only involves the elastic properties of the DMPC membranes.

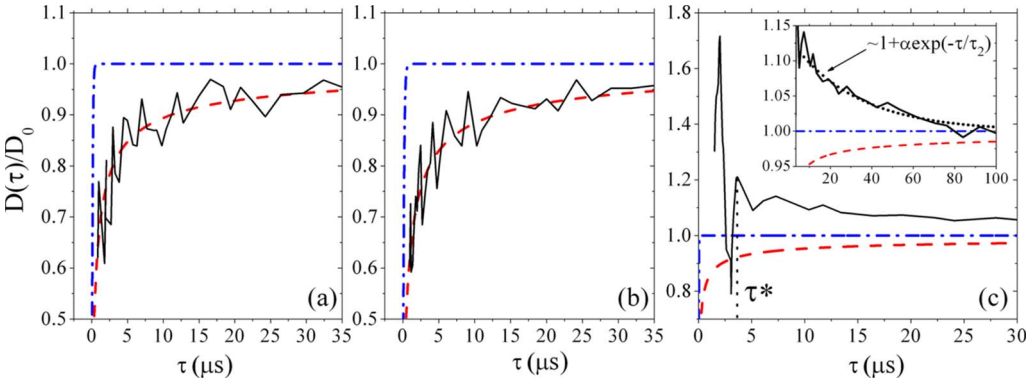

FIG. 1. (Color online) Normalized time-dependent diffusion coefficient $D(\tau)/D_0$ corresponding to sample R at (a) 13 and (b) 25 °C, and sample D at 25 °C (c). Blue dash-dotted line stands for Langevin's model: $D(\tau)/D_0=(d\langle\Delta x^2(\tau)\rangle/d\tau)/2D_0$ [Eq. (2)]. Red dashed line corresponds to the full hydrodynamic model: $D(\tau)/D_0=(d\langle\Delta x^2(\tau)\rangle/d\tau)/2D_0$ [Eq. (3)]. Black solid line represents the experiment: $D(\tau)=D_{\exp}(\tau)$. D_0 is the experimental free diffusion coefficient corresponding to each temperature. Inset in (c): dotted line represents the predicted exponential relaxation corresponding to $\tau_2=32$ μs and $\alpha=0.1$.

$D_{\exp}(\tau)$ corresponding to sample RD at 15 °C, 23 °C, and 34 °C are shown in Figs. 2(a)–2(c). In accord with our calorimetric determination, sample RD at 15 °C is associated to the rigid gel phase of the DMPC membranes. In fact, the full hydrodynamic model and the experimental data show again a common tendency as in the case of sample R [Fig. 2(a)]. At 23 °C, that is, at the main transition temperature, a moderated agreement between theory and experiment still persists although the fluctuations in $D_{\exp}(\tau)$ appear more pronounced [Fig. 2(b)]. At 34 °C the deformable crystalline phase of the lipid membranes is expected, and indeed a noticeable change in the trend shown by $D_{\exp}(\tau)$ occurs [Fig. 2(c)]. As in the case of sample D, we observe a nonmonotonic behavior of $D_{\exp}(\tau)$ with a clear maximum at very short times ($\tau^*\approx 0.6$ μs). However, sample RD presents a faster final relaxation than that associated to sample D, almost recovering its diffusive value around $\tau\approx 5$ μs.

In our opinion, the complex experimental patterns shown in Figs. 1(c) and 2(c) reflect the intricate interplay between the translational and the deformational motion of our flexible particles. At short times, when the translational velocity has not yet been damped, $D_{\exp}(\tau)$ would contain simultaneously the translational and the deformational displacements of the liposomes membrane. Thus, the strong fluid-membrane interaction due to the translational velocity would induce fast changes in the membrane's motion that would be elastically restored, being manifested through the sharp oscillations of $D_{\exp}(\tau)$. In the absence of a dynamic model for $D_{\exp}(\tau)$ in which both translational and deformational motions are considered simultaneously, the latter cannot be easily isolated to be described quantitatively. However, at long times, when the translational velocity is damped, the final relaxation of $D_{\exp}(\tau)$ toward D_0 would reflect essentially the underlying overdamped deformations in the liposome's form.

Since we have chosen an adequate q-value for our experiments ($q_f a_{\text{liposome}}\approx 6$), see for details Ref. [25], we are able to explore if this hypothetical deformational motion is present in $D_{\exp}(\tau)$, attempting to reveal the internal modes of deformation of our flexible particles [26,27]. Hence, we adopt the model proposed by Milner and Safran [26] to describe the small shape fluctuations of a single vesicle in thermal equilibrium, where the translational motion is not considered. Accordingly, the relative displacement of the membrane, $r(\tau,\Omega)$, is expanded into spherical harmonics, $Y_{lm}(\Omega)$, around a fixed radius a: $r(\tau,\Omega)=a(1+\Sigma_{l>1,m}\, u_{lm}(\tau)Y_{lm}(\Omega))$, where Ω is the solid angle and $u_{lm}(\tau)$ the amplitude associated to a given mode. By appealing the fluctuation-dissipation theorem, the auto-

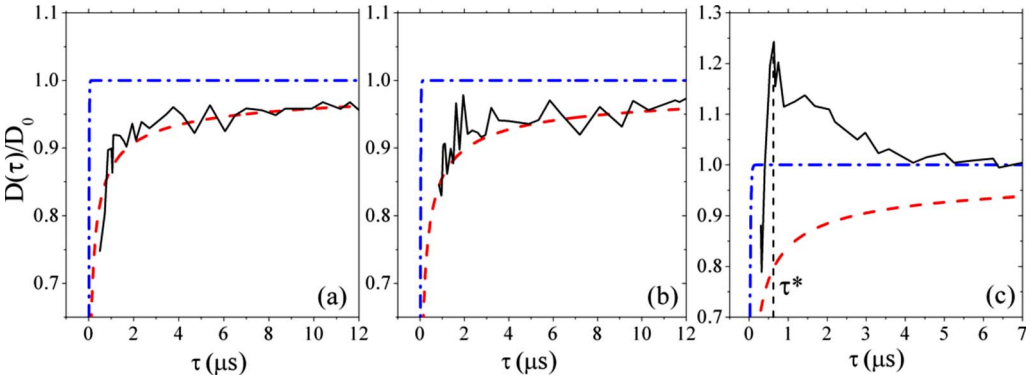

FIG. 2. (Color online) Normalized time-dependent diffusion coefficient $D(\tau)/D_0$ corresponding to sample RD at (a) 15, (b) 23, and (c) 34 °C with symbols as in Fig. 1.

correlation functions of the amplitudes present an exponential decay $\langle u_{lm}(\tau)u_{lm}(0)\rangle=\langle|u_{lm}(\tau)|^2\rangle\exp(-\tau/\tau_l)$, where the relaxation time, τ_l, of a mode driven by bending forces (negligible surface tension [26,27]) is

$$\tau_l=\frac{\eta a^3(2l+1)(2l^2+2l+1)}{k_c l^2(l+1)^2(l+2)(l-1)}, \tag{5}$$

with k_c being the bending modulus of the membranes. According to Eq. (5), the slowest relaxation is expected for the second deformational mode. Restricting ourselves to the $l=2$ contribution [25,27], the final relaxation of $D_{\exp}(\tau)$ would be in first approximation described by an overdamped exponential decay of the form $D(\tau)\approx D_0[1+\alpha\exp(-\tau/\tau_2)]$, where the damping is mediated by τ_2 as in the case of $\langle u_2(\tau)u_2(0)\rangle$. Here we implicitly assume a small deformations regime, $\langle|u|^2\rangle^{1/2}\leq 0.1$, according to the theoretical prediction for standard k_c values of the lipid membranes [26,28]. In particular, taking the bending modulus of the SPC membranes as $k_c=(1.5\pm 0.5)\cdot 10^{-19}$ J [28], the relaxation time for a vesicle of $a=244$ nm suspended in water at 25 °C is $\tau_2\approx 32$ μs [Eq. (5)]. Using this value, our exponential approximation provides a good description of the final relaxation of $D_{\exp}(\tau)$ even for amplitudes as big as $\alpha\approx 0.1$ [see inset, Fig. 1(c)]. This agreement is certainly encouraging, since it supports quantitatively our interpretation of the relaxation of $D_{\exp}(\tau)$ in terms of an overdamped deformational motion. Regarding sample RD, due to their strong temperature and membrane composition dependence, values for k_c that typically range $(2\cdot 10^{-19},\ 6\cdot 10^{-19})$ J have been documented for the DMPC membranes at the liquid crystalline phase [29]. Accordingly, the corresponding τ_2-range for a vesicle of $a=240$ nm suspended in water at 34 °C results $\tau_2\approx(6,19)$ μs. Although slightly overestimated, this prediction is also in reasonable accord with that observed for the final relaxation time of sample RD, which reaches the diffusive regime around $\tau\approx 5$ μs [see Fig. 2(c)]. These results concerning our flexible particles are the quantitative observation of the damped deformational motion of a large vesicle under spontaneous nondiffusive Brownian motion. As a result, a powerful practical application emerges: Our methodology is useful to estimate and predict the elastic properties of a great variety of biological deformable particles.

In conclusion, we have revealed the complex scenario present in the nondiffusive motion of a deformable Brownian particle, which is mediated by the coupling between translational and deformational degrees of freedom. As opposed to rigid particles, a complete theoretical understanding of this motion, including its short times description, remains as a challenge.

The authors are grateful to "MICINN" (Projects No. MAT2006-12918-C05-01-02 and No. -05), ERDF Funds, and "Junta de Andalucía" (Project P07-FQM-02496) for financial support. We thank Walter Kob for valuable comments on our manuscript.

[1] P. N. Pusey, in *Colloidal Suspension*, Proceedings of the Les Houches Summer School of Theoretical Physics, LI, 1989 (North-Holland, Amsterdam, 1989).
[2] G. Nägele, Phys. Rep. **272**, 215 (1996).
[3] J. T. Padding and A. A. Louis, Phys. Rev. E **74**, 031402 (2006).
[4] A. Einstein, Ann. Phys. **322**, 549 (1905).
[5] P. Langevin, C. R. Acad. Sci. Hebd Seances Acad. Sci. D **146**, 549 (1908).
[6] G. E. Uhlenbeck and L. S. Ornstein, Phys. Rev. **36**, 823 (1930).
[7] B. J. Alder and T. E. Wainwright, Phys. Rev. Lett. **18**, 988 (1967).
[8] B. J. Alder and T. E. Wainwright, Phys. Rev. A **1**, 18 (1970).
[9] R. Zwanzig and M. Bixon, Phys. Rev. A **2**, 2005 (1970).
[10] A. Widom, Phys. Rev. A **3**, 1394 (1971).
[11] E. J. Hinch, J. Fluid Mech. **72**, 499 (1975).
[12] C. D. Andriesse, Phys. Lett. **33A**, 419 (1970).
[13] K. Carneiro, Phys. Rev. A **14**, 517 (1976).
[14] A. Boullier, J. P. Boon, and P. Deguent, J. Phys. **32**, 159 (1978).
[15] G. L. Paul and P. N. Pusey, J. Phys. A **14**, 3301 (1981).
[16] K. Ohbayashi, T. Kohno, and H. Utiyama, Phys. Rev. A **27**, 2632 (1983).
[17] D. A. Weitz, D. J. Pine, P. N. Pusey, and R. J. A. Tough, Phys. Rev. Lett. **63**, 1747 (1989).
[18] J. X. Zhu, D. J. Durian, J. Muller, D. A. Weitz, and D. J. Pine, Phys. Rev. Lett. **68**, 2559 (1992).
[19] B. Lukić, S. Jeney, C. Tischer, A. J. Kulik, L. Forro, and E. L. Florin, Phys. Rev. Lett. **95**, 160601 (2005).
[20] R. Lipowsky and E. Sackmann, *Structure and Dynamics of Membranes* (Elsevier, New York, 1995), Vol. 1.
[21] W. D. Davenport and W. L. Root, *Random Signals and Noise* (McGraw-Hill, New York, 1958).
[22] A. Moussaïd and P. N. Pusey, Phys. Rev. E **60**, 5670 (1999).
[23] S. Roldán-Vargas, R. Barnadas-Rodriguez, M. Quesada-Perez, J. Estelrich, and J. Callejas-Fernandez, Phys. Rev. E **79**, 011905 (2009).
[24] V. P. Torchillin and V. Weissing, *Liposomes, a Practical Approach* (Oxford University Press, New York, 2003).
[25] J. S. Huang, S. T. Milner, B. Farago, and D. Richter, Phys. Rev. Lett. **59**, 2600 (1987).
[26] S. T. Milner and S. A. Safran, Phys. Rev. A **36**, 4371 (1987).
[27] R. Joannic, L. Auvray, and D. D. Lasic, Phys. Rev. Lett. **78**, 3402 (1997).
[28] M. B. Schneider, J. T. Jenkins, and W. W. Webb, J. Phys. (Paris) **45**, 1457 (1984).
[29] P. Méléard *et al.*, Biophys. J. **72**, 2616 (1997).